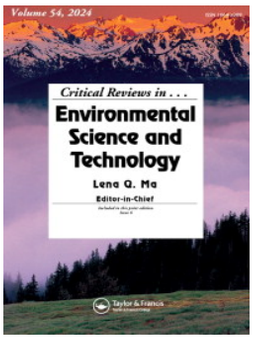

Taylor & Francis
Taylor & Francis Group

Critical Reviews in Environmental Science and Technology

ISSN: (Print) (Online) Journal homepage: www.tandfonline.com/journals/best20

Tree rings recording historical atmospheric mercury: A review of progresses and challenges

Xu Liu, Xun Wang, Wei Yuan, Dingyong Wang & Xinbin Feng

To cite this article: Xu Liu, Xun Wang, Wei Yuan, Dingyong Wang & Xinbin Feng (2024) Tree rings recording historical atmospheric mercury: A review of progresses and challenges, Critical Reviews in Environmental Science and Technology, 54:6, 445-462, DOI: 10.1080/10643389.2023.2250706

To link to this article: https://doi.org/10.1080/10643389.2023.2250706

CRITICAL REVIEWS IN ENVIRONMENTAL SCIENCE AND TECHNOLOGY
2024, VOL. 54, NO. 6, 445–462
https://doi.org/10.1080/10643389.2023.2250706

Tree rings recording historical atmospheric mercury: A review of progresses and challenges

Xu Liu[a], Xun Wang[b], Wei Yuan[b], Dingyong Wang[a] and Xinbin Feng[b]

[a]College of Resources and Environment, Southwest University, Chongqing, China; [b]State Key Laboratory of Environmental Geochemistry, Institute of Geochemistry, Chinese Academy of Sciences, Guiyang, China

ABSTRACT

Foliage uptake of atmospheric elemental mercury (Hg^0) and subsequent translocation by the phloem is the main pathway for Hg accumulation in tree rings. Tree rings have been used as the emerging natural archive to directly reconstruct centennial trends of atmospheric Hg^0 level. The tree-ring Hg records in remote regions have successfully reconstructed the peak of anthropogenic Hg emissions in Europe and North America in 1960s – 1970s and the distinct increase of Hg emissions in Asia since 1980s. Combining the Hg concentrations and isotopic signatures would provide historical atmospheric Hg trends and Hg emission source shifts. The mechanisms for Hg translocation, specifically the radial translocation and impacts of environmental and tree physiological factors, are yet to be clarified to explain the nonlinear relation between atmospheric Hg^0 concentration and Hg signals in tree rings. Thus, we recommend to trace Hg accumulation and translocation processes and their Hg isotopic fractionation in tree rings, and examine the relationship between tree-ring Hg profile and atmospheric pollution level in specific tree species. Finally, we suggest to develop more statistical models to quantify environmental and tree physiological impacts on Hg accumulation and translocation in tree rings.

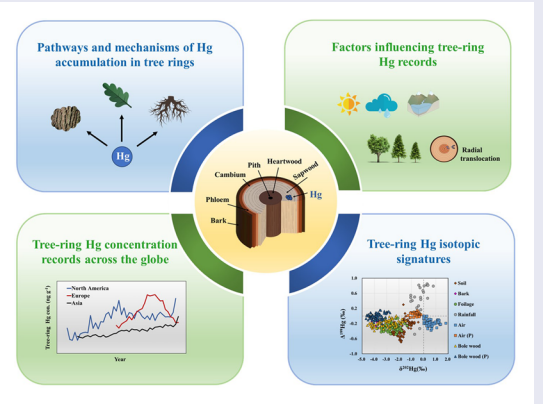

KEYWORDS Mercury; isotopes; tree rings; influencing factors; historical record

HANDLING EDITORS Dan Tsang and Lena Q. Ma

1. Introduction

Mercury (Hg) is a toxic metal and released into the atmosphere through various natural and anthropogenic processes (Beckers & Rinklebe, 2017; Horowitz et al., 2014). A cumulative total of 470 Gg Hg has been directly emitted into the atmosphere from anthropogenic sources since 1850s, 74% of which was in the form of elemental Hg (Streets et al., 2017). Gaseous elemental Hg (Hg^0) is the main form of Hg in the atmosphere with a 0.3- to 1.5- year atmospheric residence time (Chen et al., 2018; Lehnherr, 2014; Shah et al., 2021). The distinct increase of Hg emissions since 1850s have resulted in a significant elevation of Hg accumulation in remote ecosystems (Chen et al., 2014; Yu et al., 2022). The deposited Hg can be transformed into the

CONTACT Xun Wang wangxun@mail.gyig.ac.cn State Key Laboratory of Environmental Geochemistry, Institute of Geochemistry, Chinese Academy of Sciences, Guiyang 550081, China
Supplemental data for this article can be accessed online at https://doi.org/10.1080/10643389.2023.2250706.

more toxic form (i.e., methyl-Hg) in certain environments, posing distinct threat to environmental quality and human health (Evans et al., 2013; Zhang et al., 2014). To protect environment and human health from Hg pollution, the UN's Minamata Convention on Hg has entered into force in August 2017 (UNEP, 2019). Reconstructing the historical atmospheric Hg trend is the foundation to understand the Hg accumulation and transportation among the global Hg reservoirs (Cooke et al., 2020; Sonke et al., 2023).

Monitoring of atmospheric Hg^0 concentration began only 30–40 years ago, and the absence of long-term observation data has limited our capacity in assessing historical atmospheric Hg pollution and verifying historical Hg emission inventories (Clackett et al., 2018; Cooke et al., 2020). The natural archive yields a unique opportunity to provide long-term and large-scale information on atmospheric Hg concentration and deposition, thus directly linking the trend of current and past atmospheric Hg changes (Cooke et al., 2020). Ice cores (Eyrikh et al., 2017; Schuster et al., 2002), peat bogs (Enrico et al., 2017; Zuna et al., 2012), and lake sediments (Engstrom et al., 2014; Kang et al., 2016) are readily available proxy to reconstruct past trends of atmospheric Hg deposition. However, these archives are mainly found under the specific climatic and geological conditions (Cooke et al., 2020; Kang et al., 2022; Novakova et al., 2021), and rely on radioisotope dating methods (e.g., ^{14}C, ^{137}Cs and ^{210}Pb), which have several shortages such as high sampling cost, multiple factor impacts, and low temporal resolution (e.g., 10- to 50- year) (Clackett et al., 2018; Cooke et al., 2020).

Natural growth characteristics of trees enables tree rings to have several advantages for as archives of Hg deposition. These advantages include broad distribution, easy collection and replication, potential for centennial-length chronologies, and annual resolution based on the annual ring counting and cross-dating verification (Clackett et al., 2018; Kang et al., 2022; Novakova et al., 2021). Additionally, compared to other natural archives recording atmospheric deposition, tree rings directly record the signal of atmospheric Hg concentration (Arnold et al., 2018). Given the aforementioned promising advantages, tree rings have been successful used to reconstruct historical variations of atmospheric Hg concentration in remote regions (Abreu et al., 2008; Clackett et al., 2018; Eccles et al., 2020; Ghotra et al., 2020; Gustin et al., 2022a; Kang et al., 2022; Maillard et al., 2016; Navrátil et al., 2018; Peckham et al., 2019a; Wright et al., 2014).

The fundamental assumption of the Hg dendrochemistry is that Hg accumulated in tree rings is derived from atmospheric Hg sources, and a linear relationship between Hg in air and in tree rings exists (Wang et al., 2021b). Thus, atmospheric Hg concentration can be estimated from tree-ring Hg profile as follows:

$$Hg_{air(t)} = Hg_{tr(t)} \times r \tag{1}$$

where $Hg_{air(t)}$ is the estimated atmospheric Hg concentration (ng m^{-3}) for the specific period (t), $Hg_{tr(t)}$ is the simultaneous Hg concentration in a tree ring segment (ng g^{-1}), and r is the atmospheric Hg accumulation rate factor. Noteworthy, the Hg dendrochemistry is still an emerging field of research with significant knowledge gaps on the reliability of tree-ring records, such as the specific source contribution, age effect, radial translocation (Chellman et al., 2020; Novakova et al., 2021; Wang et al., 2021b). Specifically, the uncertainties of atmospheric Hg accumulation rate factor (r) reduce the reliability of tree-ring Hg records. Several studies estimated r by assuming a linear correlation between Hg in air and in tree rings (Navrátil et al., 2018; Novakova et al., 2022). However, other studies suggested a nonlinear Hg accumulation rate in tree rings due to interactions between trees and environmental factors as well as the influence of tree physiological factors on Hg uptake and translocation inside a tree (Gustin et al., 2022a; 2022b; Kang et al., 2022; Liu et al., 2024; McLagan et al., 2022; Wang et al., 2021b).

The primary objective of this review is to systematically summarize the current progresses and challenges for tree rings as the atmospheric Hg archive. We synthesized mechanisms of Hg uptake, translocation and their isotopic fractionations in tree rings, and re-assessed tree-ring Hg

profile data across the globe based on the literatures published in the last decade, and finally provided future recommendations to improve the reliability of tree-ring Hg reconstruction.

2. Pathways and mechanisms of Hg accumulation in tree rings

There are three potential sources for Hg accumulation in tree rings including atmospheric Hg uptake through foliage and then subsequent translocation by phloem, atmospheric Hg absorption by bark and then lateral transmission into tree rings, and soil Hg absorption by root then upward transportation by xylem (Navrátil et al., 2018; Novakova et al., 2022; Wang et al., 2021b; Yuan et al., 2022). Quantifying the contributions from these sources would significantly improve the accuracy of estimating atmospheric Hg concentration from tree-ring Hg records (Figure 1).

2.1. Foliage uptake of atmospheric Hg^0 and then translocation into tree rings

Measurements of air-foliage Hg exchange flux (Fleck et al., 1999; Millhollen et al., 2006) and stable Hg isotopic signatures (Graydon et al., 2009; Mao et al., 2013; Yuan et al., 2019) have shown that approximately 90% of Hg in foliage was derived from atmospheric Hg^0 uptake. There are two pathways for foliage assimilation of atmospheric Hg^0 (Figure 1). One pathway is *via* stomatal uptake of atmospheric Hg^0 (Assad et al., 2016; Laacouri et al., 2013; Stamenkovic & Gustin, 2009; Yuan et al., 2019). Stomata are responsible for the exchange of CO_2, O_2 and H_2O between air and foliage during respiration and photosynthesis, and also passively exchange various gaseous pollutants including Hg^0 (Frescholtz et al., 2003; Liu et al., 2021a). The stomatal conductance significantly shapes the rate of foliar atmospheric Hg^0 uptake during the daytime (Arnold et al., 2018; Converse et al., 2010; Stamenkovic & Gustin, 2009). The other pathway is the nonstomatal uptake, which is suggested dominant at night (Stamenkovic & Gustin, 2009; Zhang et al., 2009). It is likely that foliage cuticles involve in the nonstomatal route (Arnold et al., 2018; Laacouri et al., 2013). Cuticles contain both polar and nonpolar routes, and enable to let both Hg^0 (nonpolar) and Hg^{2+} (polar) pass through the cuticle (Arnold et al., 2018; Stamenkovic & Gustin, 2009).

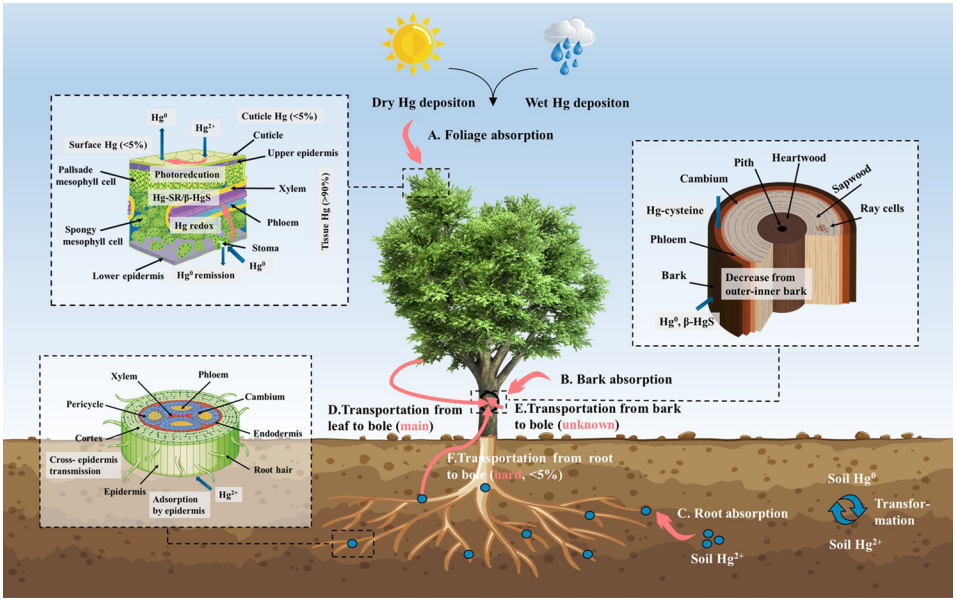

Figure 1. Schematic diagram of Hg accumulation in tree issues.

After uptake by foliage, Hg^0 undergoes oxidation inside foliage *via* a two-step single electron transfer process, involving Hg^+ and Hg^{2+} formation mediated by nonenzymatic and enzymatic (e.g., catalase) reactions (Liu et al., 2021b). Hg^0 oxidation to Hg^+ is demonstrated as a nonenzymatic reaction. Subsequently, the oxidated Hg^{2+} is incorporated in epidermal and stomatal cell walls, as well as in parenchyma cell nuclei or adsorbed to outer leaf surfaces (Laacouri et al., 2013; Stamenkovic & Gustin, 2009). Up to 96% of Hg is accumulated in the leaf tissue compartment, while 4-5% of Hg in cuticle compartments and leaf surface (Laacouri et al., 2013). Hg complexes formed with the reduced sulfur functional groups (Hg-SR), bis-thiolate complex ($Hg(SR)_2$) and Hg sulfide nanoparticles (β-HgS) have been identified as the dominant Hg species in foliage due to the high Hg affinities of the thiol functional group (-SH) and reduced sulfur functional groups (-SR) (Carrasco-Gil et al., 2013; Liu et al., 2021a; Manceau et al., 2018).

The nutrient translocation incidentally moves metal-ligand complexes with low molecular compounds containing Hg from canopy to stem (Arnold et al., 2018; Gustin et al., 2022a; Navratil et al., 2017). Stable Hg isotopic signatures (Wang et al., 2020a) and results from the controlled dose-response experiment (Arnold et al., 2018) and field control experiment (Peckham et al., 2019b) have shown that approximately 80% of Hg in tree rings derived from foliage uptake of atmospheric Hg^0 and subsequent translocation by the phloem. Additionally, Hg concentrations in biomass of stem significantly increased along with the height of stem, which also reflected the Hg transport from canopy to woody biomass after foliage uptake of atmospheric Hg^0 (Liu et al., 2024; Yanai et al., 2020).

2.2. Bark absorption of Hg

Bark absorption of Hg may also contribute to the Hg accumulation in tree rings (Figure 1). Bark can effectively absorb airborne pollutants including Hg due to its porous morphology and lack of metabolic activity (Şen et al., 2015). Particle-bound Hg and Hg^0 are considered to be the original species deposited onto the barks by interaction with the surrounding atmosphere (Chiarantini et al., 2017). Stable Hg isotopic evidences suggested that the foliage uptake of atmospheric Hg^0, then internal translocation from phloem to inner bark also probably contribute to Hg accumulation in bark (McLagan et al., 2022). The bark Hg concentration is usually one order of magnitude greater than concentration in tree rings (more details in Table S1) (Kang et al., 2019; Novakova et al., 2021; Rodriguez Martin et al., 2013; Siwik et al., 2010; Zhou & Obrist, 2021). The elevated Hg concentration in the outmost ring is speculated by Hg lateral translocation from tree bark to ring (Kang et al., 2019; Novakova et al., 2022). However, the rapid decrease of Hg concentration from outer-to-inner bark (Table S1) indicates the inefficiency of Hg passing through multiple layers of bark to enter into xylem (Chiarantini et al., 2016; Novakova et al., 2021).

2.3. Root absorption of soil Hg

Hg^{2+} bound with lower molecular organic matter (such as cysteine) in a surrounding soil solution is suggested as the main source for Hg in roots (Wang et al., 2012; Yuan et al., 2022). It has been well documented that up to 90% Hg in the root zone is tightly bound to membranes of roots and cell walls, and only a small amount of Hg in roots (<5%) can be translocated into the aboveground woody biomass (Cui et al., 2014; Greger et al., 2005; Millhollen et al., 2006; Wang et al., 2012; Yuan et al., 2022) due to the low bioavailability of Hg and barrier block in roots (Bishop et al., 1998; Boszke et al., 2008; Wang et al., 2012; Yuan et al., 2022). The controlled experimental results showed that tree-ring Hg concentrations of Pinus trees were primarily influenced by air Hg concentrations but not soil Hg concentrations (Arnold et al., 2018; Peckham et al., 2019b). Results from the Hg isotopic mixing models further indicated that atmospheric Hg^0 accounted for 83-88% in bole wood

(Wang et al., 2020a). Thus, the soil Hg absorption by root is not the main Hg source in tree rings.

3. Tree physiological factors influencing tree-ring Hg records

Tree physiological processes control foliage uptake of atmospheric Hg^0 and the subsequent translocation and accumulation in aboveground biomass, thus significantly influencing the Hg profile in tree rings (Figure 2). These physiological factors include but are not limited to the stomatal characteristic, epidermal composition, leaf area, xylem properties, transpiration rate and canopy dynamics (Arnold et al., 2018; Chellman et al., 2020; Laacouri et al., 2013; Peckham et al., 2019a; Schneider et al., 2019). Currently, few studies have provided direct evidences to display impacts of tree physiological factors on tree-ring Hg accumulation. Herein, we mainly discussed tree species, tree age and radial translocation, which likely represent the comprehensive impacts of tree physiological factors on Hg accumulation in tree rings.

3.1. Tree species

Compared to broadleaf tree species, coniferous tree species are more conducive to ring dating due to their clearer ring boundaries and fewer false rings and fractures (Gustin et al., 2022a; Siwik et al., 2010). Previous studies had different assessments on the suitability of using broadleaf tree rings as archives for atmospheric Hg pollution trends. For example, Siwik et al. (2010) found insignificant temporal variations of tree-ring Hg profiles in broadleaf tree species, such as Red oak (*Quercus rubra*), Poplar (*Populus deltoides*) and Willow *(Salix rubens)*; while Maillard et al. (2016) proposed that tree-ring Hg profiles of Poplar and Willow could record historical

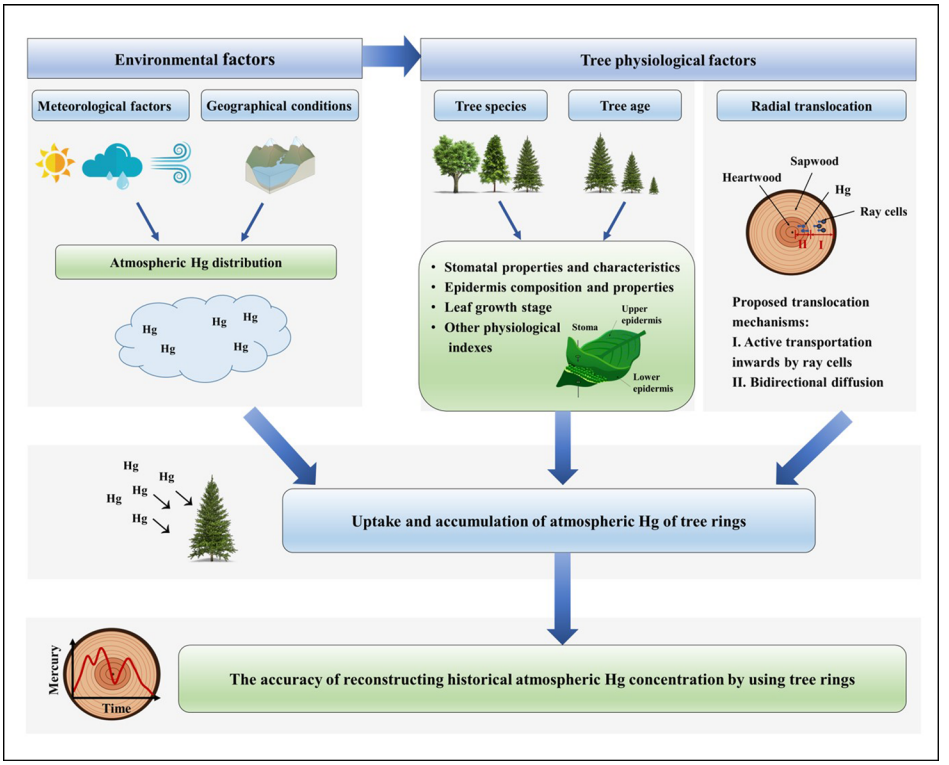

Figure 2. Factors affecting reconstruction of atmospheric Hg concentration by tree rings. The arrow indicates the effects of one factor on another.

Hg emissions from past industrial activities. For coniferous tree species, number of studies have demonstrated that the tree-ring Hg profiles in coniferous tree species, such as *Pinus* spp. (Gustin et al., 2022a; Peckham et al., 2019a; Schneider et al., 2019; Wright et al., 2014), *Picea* spp. (Clackett et al., 2018; Eccles et al., 2020; Kang et al., 2018) and European larch (*Larix decidua Mill.*) (Navrátil et al., 2018; Novakova et al., 2021), are preferential for Hg dendrochronology, specifically as a relevant proxy of anthropogenic Hg emissions in polluted areas.

Among the coniferous tree species, the evergreen pines possibly have the elevated tree-ring Hg concentration in contrast to the deciduous pines, as indicated by several field observations. The mean Hg concentration in tree-ring cores of Scots pine (90- to 220-year-old, *Pinus sylvestris*) at three background sites in Czech Republic was 1-2 times higher than that of mature European larch (80- to 130-year-old, *Larix decidua Mill.*) (Novakova et al., 2021). Similarly, the Hg concentration in tree-ring cores of mature (about 200-year-old) Mongolian pine (1.98 ± 0.39 ng g^{-1}, *Pinus sylvestris var. mongolica*) was higher than that in mature (about 150-year-old) Dahurian larch (1.51 ± 0.48 ng g^{-1}, *Larix gmelinii Rupr.*) at the same sampling site (Kang et al., 2022). Besides the differences in physiological processes, deciduous needles only grow in summertime, resulting in only 4-6 months of foliage exposure to atmospheric Hg^0, in contrast to the whole year growth of evergreen needles (Kang et al., 2022; Novakova et al., 2021). Thus, the tree-ring Hg profile of deciduous pines possibly reflect the trend of summertime atmospheric Hg^0 concentration, and Hg profile of evergreen needle trees may reflect the average atmospheric Hg^0 concentration across the whole year (Scanlon et al., 2020).

Among the evergreen coniferous tree species, Hg concentrations in tree rings also seem to be species-specific. For example, Hg concentration of mature (more than 200-year-old) Huon pine (9.1 ± 5.1 ng g^{-1}, *Lagarostrobus franklinii*) was higher than that of mature (more than 200-year-old) Celery top pine (3.5 ± 1.7 ng g^{-1}, *Phyllocladus aspleniifolius*) at the same sampling site in Tasmania, Australia (Schneider et al., 2019). Such a difference can be attributed to the different stomatal position and epidermal properties between these tree species. Stomata in Huon pine are well disseminated over the outer (exposed) surface of the leaf, while those in Celery top pine are dominantly on the lower surface of the phyllodes (Schneider et al., 2019). The waxy surface of celery top pine phyllodes also constrains Hg uptake by stomata (Schneider et al., 2019).

3.2. Tree age

Tree age is a straightforward parameter obtained from tree-ring counting, and is a valuable indicator to reflect the comprehensive impacts of canopy structure, tree height, stomatal conductance and epidermal properties (England & Attiwill, 2006;; Peckham et al., 2019a; Stoffberg et al., 2008). The tree-ring Hg concentrations of young trees might be higher than those of mature trees at the same location during the common growth period (Liu et al., 2024; Peckham et al., 2019a; Wang et al., 2021b). For example, Wang et al. (2021b) reported that the tree-ring Hg concentrations of young Masson pine (*Pinus massoniana*) trees (40- to 50-year-old) are 1–7 times higher than those of mature trees (more than 100-year-old) during the same growth period. There are several possible causes for such an age effect. The first one is because foliage of young trees has greater capacity of assimilating atmospheric Hg due to its higher stomatal conductance and enzyme (e.g., catalase) activity compared to foliage of mature trees (Hubbard et al., 1999; Peckham et al., 2019a). The second cause could be the decreasing rate of cuticular Hg uptake with increasing tree age because the absorption sites in cuticles are opt to saturation in the aged tissues (Schneider et al., 2019; Schreiber, 2005). Thirdly, the lower canopy heights of young trees than mature trees imply shorter distances for Hg translocation from canopy to the stem, thus causing the elevated Hg concentration in tree rings of young trees (Liu et al., 2024; Wang et al., 2021a; Yanai et al., 2020).

3.3. Radial translocation

Radial translocation of an element is defined as a change or lateral re-equilibrium in concentration within growth rings previously formed because the element is moved or smeared across active growth rings (Arnold et al., 2018; Cheng et al., 2007; Hagemeyer & Schafer, 1995; Stewart, 1966; Watmough & Hutchinson, 2002). Such a centripetal translocation of toxic substances *via* the rays into the heartwood was a possible detoxification mechanism of living tissues in the outer sapwood (Hagemeyer & Schafer, 1995; Lageard et al., 2008). The radial translocation of Hg mainly occurs throughout the sapwood rings (Cutter & Guyette, 1993; Okada et al., 2012) since the active and live ray cells in the sapwood rings that allow water and nutrients to move radially may possibly transport Hg inwards (Arnold et al., 2018; Siwik et al., 2010). The Hg radial translocation would severely alter the atmospheric Hg signal preserved in tree rings formed in previous years. For example, the tree-ring Hg profile in Masson pine even displayed an opposite trend in contrast to the trend of local anthropogenic Hg emissions (Liu et al., 2024).

The impact of radial translocation on tree-ring Hg record is species-specific due to the heterogeneity of sapwood-heartwood distribution (Novakova et al., 2021). The narrow sapwood and heartwood with low moisture and permeability would largely constrain the radial translocation, such as tree species of *Larix* spp. and *Picea* spp. (Clackett et al., 2021;; Eccles et al., 2020; Ghotra et al., 2020; Kang et al., 2018; Navrátil et al., 2018; Novakova et al., 2021). In contrast, *Pinus* spp. and *Poplar* spp. have a wide sapwood, which leading to a strong Hg radial translocation capability (Arnold et al., 2018; Chellman et al., 2020; Gustin et al., 2022b; Liu et al., 2024; Novakova et al., 2021; Wang et al., 2021b).

The advection-diffusion model (Chellman et al., 2020; Liu et al., 2024) provides a new way to quantify impacts of radial translocation on tree-ring Hg record although such a model has not been parameterized with a complete set of physiological processes. Results of advection-diffusion model suggested that the advection, i.e., the active transport of ray cells in the sapwood, is the main pathway for radial Hg translocation in tree rings (Chellman et al., 2020; Liu et al., 2024). Liu et al. (2024) further pointed out that stronger Hg translocation occurs in young trees because of their higher abilities for translocations of nutrient and water by ray-cell compared to mature trees. Previous studies recommended to minimize impacts of radial translocation on Hg dendrochemistry by choosing tree species with a low number of sapwood rings and a low heartwood moisture content (e.g., *Larix* spp. and *Picea* spp.), or reducing resolution (10- or 20- year) of tree rings or increasing the tree-ring cores (tree numbers ≥ 10) (Cutter & Guyette, 1993; Liu et al., 2024; Novakova et al., 2021).

4. Environmental factors influencing tree-ring Hg records

4.1. Meteorological factors

The environmental conditions including meteorological factors and geographical conditions can distinctly shape Hg migration and storage in tree rings by influencing atmospheric Hg cycling and tree physiological processes (Figure 2). Gustin et al. (2022a) reported that meteorological factors, including dew point, temperature, vapor pressure deficit and relative humidity, were negatively correlated to tree-ring Hg concentrations (r ranging from −0.80 to −0.49, $p < 0.01$). The local meteorological factors can shape the trend of tree-ring Hg *via* influencing Hg emissions from natural surfaces and atmospheric Hg cycling (Gustin et al., 2022a; Liu et al., 2024). Field observations showed that relative humidity (Zhang et al., 2015) and wind speed (Fu et al., 2010) could have a negative correlation with atmospheric Hg concentration, thus influencing the air-foliage Hg exchange flux. Additionally, trees located downwind of pollution sources could capture elevated Hg in tree rings (Schneider et al., 2019). Meteorological factors may also distinctly shape tree physiology, especially stomatal conductance, thus affecting the foliar uptake of atmospheric Hg^0 and subsequent accumulation in tree rings (Liu et al., 2024; Rutter et al.,

2011). Soil moisture and temperature can affect the efficiency of Hg uptake *via* influencing the foliage stomata open-close and translocation in tree phloem. Spruce under the low soil temperature (< 8 – 10 °C) would actively reduce tree transpiration and photosynthesis, thus decreasing stomatal uptake of Hg^0 (Schwarz et al., 1997). In addition, trees grown in high moisture soil tend to have a large stomatal conductance and elevated atmospheric Hg assimilation, thus likely resulting in a high level of Hg translocated into tree rings (Eccles et al., 2020; Wohlgemuth et al., 2022).

4.2. Geographical and geomorphological conditions

Geographical and geomorphological conditions have indirect effects on Hg accumulation and translocation in tree rings *via* their complicated roles in controlling local atmospheric circulation, Hg cycling and vegetation physiological processes. The observation in northwestern Canada depicted that the tree-ring Hg concentration of White spruce in the coastal regions can be 1-2 times of that in the same tree species of inner land regions (2.96 ± 0.45 ng g^{-1} versus 1.22 ± 0.57 ng g^{-1}) (Clackett et al., 2018; Ghotra et al., 2020). These tree-ring Hg gradients were caused by the intensive sea – land interaction induced Hg cycling. Additionally, elevation has complicated effects on tree-ring Hg profiles. Several observations displayed an elevation gradient of tree-ring Hg (Gustin et al., 2022a; Kang et al., 2018), while insignificant gradient in other montane regions (Peckham et al., 2019a) due to distinct spatial heterogeneities and changes in the geographical environment. In Hg-enriched (e.g., permafrost) or polluted soils, the biological and abiotic soil factors (e.g., methylated micro-organisms, level of organic matter and etc.) have impacts on Hg accumulation in tree rings by controlling the Hg re-emission from soil, due to the soil emitted Hg then absorbed by foliage (Kang et al., 2022; Maillard et al., 2016).

5. Tree-ring Hg concentration records across the globe

The published tree-ring Hg records at most sites have the potential to reflect the local and regional atmospheric Hg changes. The tree rings at high latitude and altitude areas may record the global background Hg change. It is noteworthy that the complicated impacts from various factors (e.g., physiological processes of tree species, meteorological factors, and geographical and geomorphological conditions) lead to tree-ring Hg records with substantial variabilities. Thus, caution should be taken and additional supporting evidence collected from other natural Hg archives (e.g., ice cores, peat cores) are needed when comparing tree-ring Hg records among different sites.

5.1. Methodology of Hg dendrochemistry

Most studies have observed high variabilities of tree-ring Hg profiles among tree individuals (Clackett et al., 2018, 2021;; Ghotra et al., 2020; Liu et al., 2024; Wang et al., 2021b). Recent studies suggested that using ~10 or more tree ring cores can remarkedly reduce such tree-specific variabilities (Liu et al., 2024; Peckham et al., 2019a). It is important to ensure choosing basically consistent tree age and sampling height of tree cores during the sampling processes (Gustin et al., 2022a; Peckham et al., 2019a; Wright et al., 2014). For analysis, the thermal decomposition, amalgamation and atomic absorption spectrometry are extensively applied to determine total Hg concentration in tree-ring cores (Clackett et al., 2018; Gustin et al., 2022a; Liu et al., 2024; Peckham et al., 2019a; Schneider et al., 2019). Due to the extremely low concentrations of Hg in tree rings in remote regions (generally lower than 5.0 ng g^{-1}), the low instrument blank must be ensured to reduce influences of background noise (Peckham et al., 2019a). Most published tree-ring Hg records are developed at 5- or 10-year resolution (Chellman et al., 2020; Clackett et al., 2018; Eccles et al., 2020; Gustin et al., 2022a; Hojdová et al., 2011; Kang et al., 2018;

Navrátil et al., 2018; Peckham et al., 2019a; Wang et al., 2021b), and several studies take full advantage of the annual resolution of the tree-ring record (Ahn et al., 2020; Clackett et al., 2021; Jung & Ahn, 2017). Most studies compiled the mean tree-ring records by calculating the arithmetic averages of all the segment concentrations (Chellman et al., 2020; Liu et al., 2024; Navratil et al., 2017; Novakova et al., 2021, 2022; Wright et al., 2014), while several studies (Eccles et al., 2020; Kang et al., 2022) calculated the Hg series using Tukey's biweight robust mean, or tree-specific bias adjusted mean (Clackett et al., 2018; Ghotra et al., 2020). These adjusted mean-calculation methods are commonly applied in dendrochronological research and unaffected by outliers, and thus well suited to small sample size and non-normally distributed data sets (Cook et al., 1990). In addition, the sparce principal component analysis (PCA) is also recommended due to it overcomes the particular disadvantage of ordinary PCA, being that the principal components are usually linear combinations of all input variables (Maillard et al., 2016).

5.2. Hg records in remote regions

Figures 3–5 synthesize the tree-ring Hg records across the globe. Existing studies reporting tree-ring Hg records are all from the Northern Hemisphere, including the United States (Chellman et al., 2020; Gustin et al., 2022b; Peckham et al., 2019a; Wright et al., 2014; Yanai et al., 2020), Canada (Clackett et al., 2018; Eccles et al., 2020; Ghotra et al., 2020), Czech Republic (Hojdová et al., 2011; Navrátil et al., 2018; Novakova et al., 2021), Germany (McLagan et al., 2022; Novakova et al., 2022), China (Kang et al., 2018; 2022; Liu et al., 2024; Wang et al., 2021b) and South Korea (Ahn et al., 2020; Jung & Ahn, 2017), except one study in Australia inform the Southern Hemisphere (Schneider et al., 2019). Tree rings in these studies are mainly focused on coniferous species including *Pinus* spp. and *Picea* spp., and some broadleaf species. Most tree-ring records cover 150-200 years of time. According to the peak of anthropogenic emissions (Streets et al., 2017), the whole record was divided into four periods as discussed below.

The first period covers 1861–1920 (I). The beginning of the industrialization led to an increase of atmospheric Hg emissions in Europe and North America. The anthropogenic Hg emissions

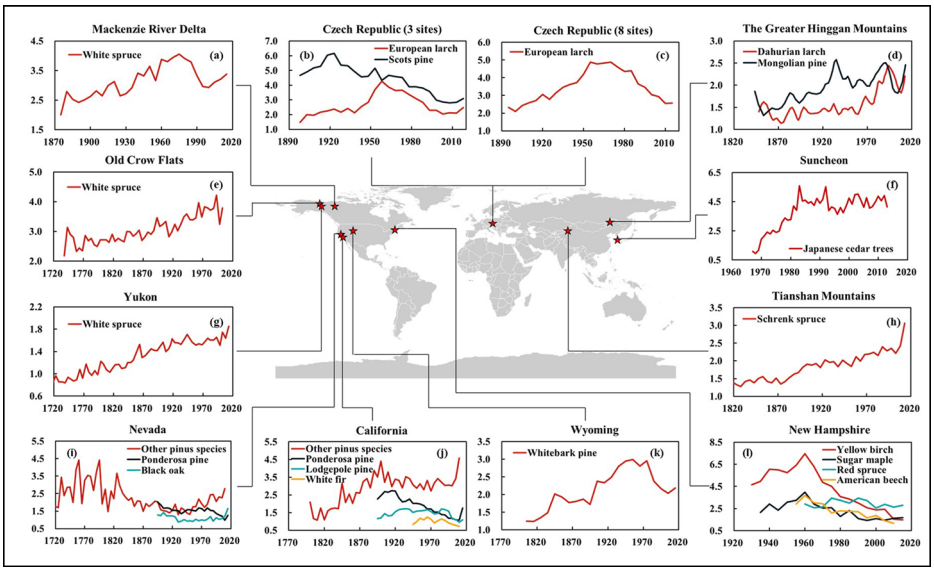

Figure 3. Records of tree-ring Hg profiles for different tree species in background regions. The abscissa presents the time covers and the ordinate displays variations of tree-ring Hg concentration (ng g^{-1}). data sources: Ahn et al., 2020; Chellman et al., 2020; Clackett et al., 2018; Eccles et al., 2020; Ghotra et al., 2020; Gustin et al., 2022a; Jung & Ahn, 2017; Kang et al., 2022; Kang et al., 2018; Novakova et al., 2021; Wright et al., 2014; Yanai et al., 2020.

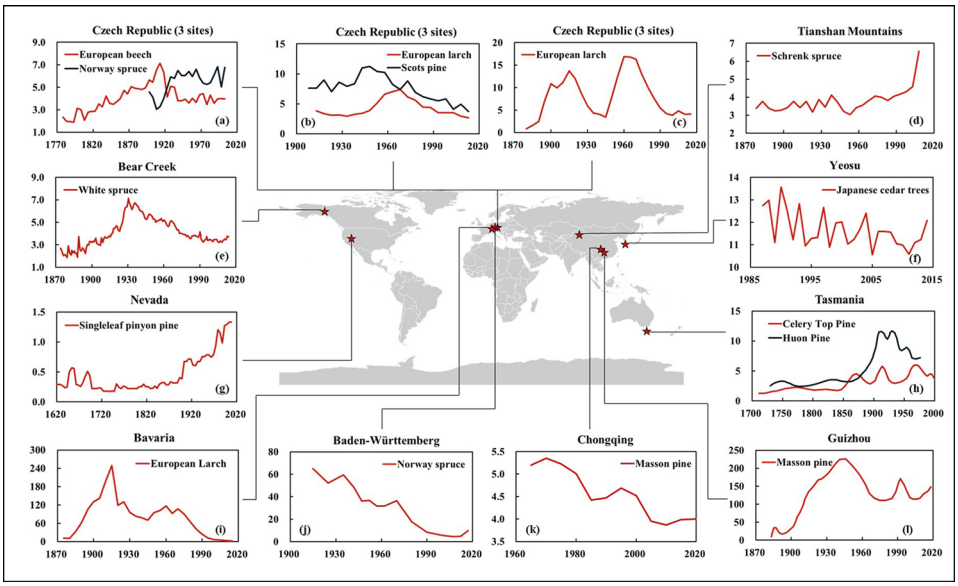

Figure 4. Records of tree-ring Hg profiles for different tree species in polluted regions. The abscissa presents the time covers and the ordinate displays variations of tree-ring Hg concentration (ng g^{-1}). data sources: Ahn et al., 2020; Clackett et al., 2021; Hojdová et al., 2011; Jung & Ahn, 2017; Kang et al., 2018; Liu et al., 2024; McLagan et al., 2022; Navrátil et al., 2018; Novakova et al., 2021; Novakova et al., 2022; Schneider et al., 2019; Wang et al., 2021b; Wright et al., 2014.

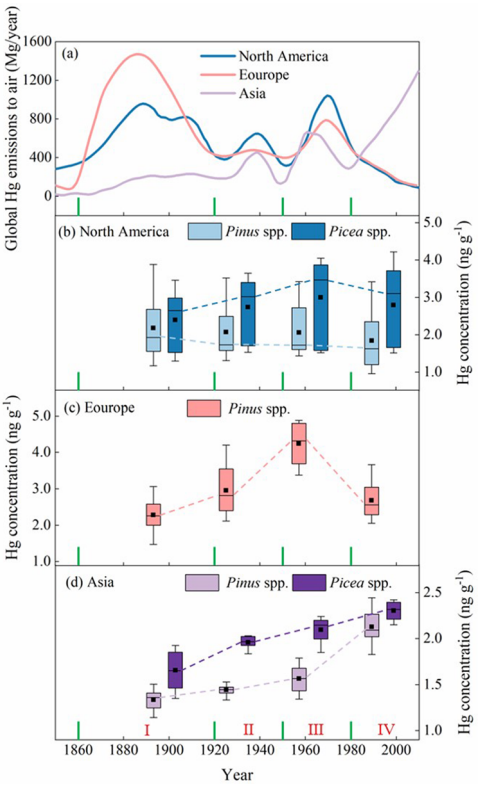

Figure 5. Temporospatial trends of anthropogenic Hg emissions and tree-ring Hg records. (a) is for anthropogenic Hg emissions from Streets et al., 2017; (b)-(d) are coniferous tree-ring Hg records in background regions of different continents.

reached a peak of 3100-3200 Mg yr^{-1} in 1890s due to the artisanal and small-scale gold and silver mining (ASGM) in North America (Streets et al., 2011, 2017). However, most tree-ring Hg records in Canada and the United States are absence of such peak in tree-ring Hg records (Figure 3(a,e,g,i,k)). The tree-ring Hg profile at one site of California reconstructed this peak (Figure 3(j)). We proposed two possible causes to explain this phenomenon. One cause is that the anthropogenic emissions from ASGM may have been overestimated due to the great uncertainties in the global use of Hg in the ASGM sector (Selin & Selin, 2022; Streets et al., 2017). Indeed, there is a lack of reliable official statistics because a large amount of the ASGM activities is unacknowledged or unregulated in many regions (Pang et al., 2022; Selin & Selin, 2022). Another cause is that Hg emissions from ASGM sector had slower release rate and weaker intensity, which might not lead to a distinct Hg rising across the globe when compared to emissions from urban-industrial activities (Guerrero, 2016).

The second period covers 1921–1950 (II). Chemicals manufacturing activities, such as chlor-alkali production, oil production, were the major Hg emission sources with a small peak (~2300 Mg yr^{-1}) in the 1940s (Streets et al., 2017). Currently, most tree-ring profiles are absence of such a peak possibly due to much smaller emission intensities than other historical peaks (Figure 3).

The third period covers 1951–1980 (III). Hg anthropogenic emissions reached another peak in the 1970s (~3000 Mg yr^{-1}) due to substantial Hg emissions from metal smelting, coal combustion, chemicals manufacturing and artisanal and small-scale gold mining in Europe and North America (Streets et al., 2017). Such a peak has been widely reconstructed in most tree-ring Hg records of White spruce in Canada (Figure 3(a)), some *Pinus* spp. and broad-leaved tree species in the United States (Figure 3(k,l)), and larch in the Czech Republic (Figure 3(b,c)).

The fourth period covers 1981–2020 (IV). Since the 1980s, the developed countries have strengthened the implementation of clean air strategies and regulations, thus largely reducing anthropogenic Hg emissions (Horowitz et al., 2014). Most tree-ring Hg records in North America and Europe showed a significant downward trend (Figure 3(a,b,c,e,j,k,l)) during this period. However, the increasing industrialization (e.g., coal combustion and metal smelting) in Asian countries contributes to a sharp increase of anthropogenic Hg emissions (Kang et al., 2018; Wu et al., 2016). The tree-ring Hg records in East Asia have confirmed this increasing trend (Figure 3(d,h)).

5.3. Hg records at polluted sites

Due to complicated impacts of emission levels and pollutant types, the tree-ring Hg concentrations at polluted sites varied widely (1–2412 ng g^{-1}), and these values are significantly higher than those in remote regions. Similar to traditional bioindicators (e.g., moss and lichen), Hg concentrations in tree rings decreased with increasing distance from the pollution sources (Jung & Ahn, 2017; Navratil et al., 2017; Novakova et al., 2022). At the temporal scale, the tree-ring Hg profiles are basically consistent with historical trends of Hg emissions from the nearby big-point Hg emission sources (Figure 4). For example, the larch tree-ring Hg profiles impacted by emissions of lead ore smelting and gold amalgamation processing in Czech Republic showed a distinctly increasing trend along with the increase of the amounts for mined ore and recovered gold in Figure 4(c) (Navrátil et al., 2018). The tree-ring Hg concentration increased sharply since 1990 due to the increasing Hg emissions from cement production and coal-fired power plant of local regions in Figure 4(d) (Kang et al., 2018). Similarly, the rapid increase of spruce tree-ring Hg from 1923 to 1930 due to the distinct Hg emissions from gold mining operations at Bear Creek camp in Figure 4(e) (Clackett et al., 2021). These results further confirmed that the suitability of tree rings to reconstruct historical atmospheric Hg levels at Hg polluted sites.

6. Tree-ring Hg isotopic signatures

Hg has seven stable isotopes (i.e., ^{196}Hg, ^{198}Hg, ^{199}Hg, ^{200}Hg, ^{201}Hg, ^{202}Hg and ^{204}Hg) in the environments (Blum & Bergquist, 2007). They undergo mixing and fractionation in the process of biogeochemistry reaction, which modifies the Hg isotope ratios in environmental samples (Kwon et al., 2020). The Hg stable isotopes have three-unique dimensions of isotopic fractionation which is quantified as the mass dependent fractionation (MDF, mainly represented by δ^{202}Hg), odd mass independent fractionation (odd-MIF, reported as Δ^{199}Hg and Δ^{201}Hg), and even mass independent fractionation (even-MIF, reported as Δ^{200}Hg and Δ^{204}Hg) (Blum & Bergquist, 2007; Sonke & Blum, 2013). The Hg stable isotopes provide a new insight in tracing Hg sources and transformation processes in natural environments. Atomoshperic Hg^0 in global background regions is generally characterized by positive δ^{202}Hg values (mean of 0.59 ± 0.44) and negative Δ^{199}Hg (mean of -0.18 ± 0.08‰); in contrast, air Hg^0 collected from urban-industrial sites displays negative δ^{202}Hg (mean of -0.62 ± 0.26‰) and near-zero Δ^{199}Hg (mean: 0.04 ± 0.05‰) values (Demers et al., 2013; Enrico et al., 2016; Kwon et al., 2020; Yuan et al., 2019). Hg in background precipitation is characterized by negative δ^{202}Hg (mean: -0.35 ± 0.58‰) and positive Δ^{199}Hg (mean: 0.45 ± 0.37‰) values (Demers et al., 2013; Enrico et al., 2016; Zhang et al., 2020; Zheng et al., 2016). Therefore, the odd-mass MIF is particularly useful in distinguishing contribution of precipitation sources characterized by positive values and atmospheric Hg^0 sources characterized by negative signals (Fu et al., 2021; Scanlon et al., 2020). The δ^{202}Hg of foliage (mean of -2.56 ± 0.48‰, ranging from -1.35 to -3.78‰) in remote forests is more negative than that of atmospheric Hg^0 (Demers et al., 2013; Guedron et al., 2018; Lu et al., 2021; Yuan et al., 2019; Zheng et al., 2016), due to a preferential uptake of lighter Hg isotopes from the atmosphere by foliage tissues (Gustin et al., 2022b; Wang et al., 2021b). The Hg odd-MIF characteristics in foliage (Δ^{199}Hg mean of -0.30 ± 0.09‰) is slightly altered by the Hg^0 re-emission from foliage (Yuan et al., 2019).

Several studies (McLagan et al., 2022; Scanlon et al., 2020; Wang et al., 2021b) have reported Hg isotopic signatures in tree rings (Figure 6). Tree-ring Hg in the remote forest is characterized by negative δ^{202}Hg (mean of -3.02 ± 0.78 ‰, ranging from -4.57 to -1.44 ‰) and negative Δ^{199}Hg (mean of -0.19 ± 0.08 ‰, ranging from -0.39 to 0.01 ‰) that broadly similar to signatures of background air Hg^0. Tree ring Hg near the pollution sites has the negative δ^{202}Hg signatures (mean of -3.83 ± 0.47 ‰, ranging from -4.61 to -2.72 ‰), while Δ^{199}Hg values (mean of 0.00 ± 0.08 ‰, ranging from -0.21 to 0.16 ‰) are closed to those observed in urban-industrial

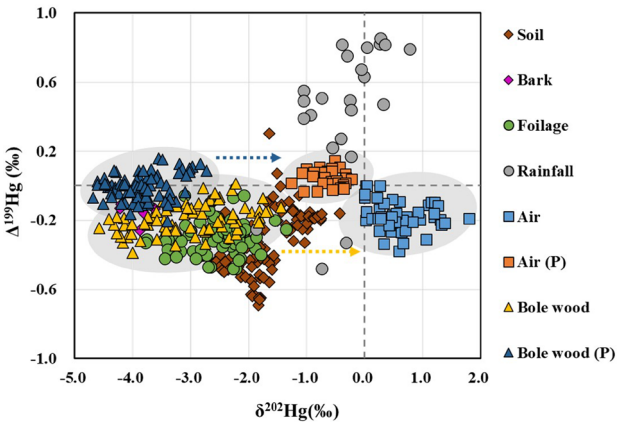

Figure 6. Mercury isotopic Compositions in forest ecosystems. P represents samples from polluted areas, and the rest samples are obtained from background areas. The δ^{202}Hg in tree-ring reflects the signal of mass dependent fractionation, and Δ^{199}Hg reflects even mass independent fractionation. Data sources: Demers et al., 2013; Enrico et al., 2016; Guedron et al., 2018; Kwon et al., 2020; Lu et al., 2021; McLagan et al., 2022; Scanlon et al., 2020; Wang et al., 2021b; Yuan et al., 2019; Yuan et al., 2020; Zhang et al., 2020; Zheng et al., 2016.

atmospheric Hg^0. The Hg isotope signatures consistently suggest that the Hg in tree rings mainly inherited from the foliar uptake of atmospheric Hg^0, rather than root absorption of deposited Hg^{2+} in soil solution (Wang et al., 2020b, 2021b; Yuan et al., 2019). The Hg uptake by foliage, downward translocation through the phloem to xylem, and subsequent radial translocation among sapwood and heartwood rings would not lead to a distinct Hg odd-MIF, but can pose complicated impacts on Hg-MDF (Kwon et al., 2020; Wang et al., 2020a).

The tree-ring Hg odd-MIF profiles have the potential to reconstruct a decadal-resolution temporal trend of the atmospheric Hg^0 and can also be used as a tracer to distinguish the emission source shifts of atmospheric Hg^0 (McLagan et al., 2022; Scanlon et al., 2020; Wang et al., 2021b). Wang et al. (2021b) observed that the average values of Δ^{199}Hg and Δ^{201}Hg presented an increasing trend during the large-scale Hg mining period, and gradually decreased after the cessation of Hg mining activities. However, there are several limitations in using Δ^{199}Hg profiles to reflect the historical Hg trends. Firstly, Δ^{199}Hg is not as sensitive as that of Hg concentration in tree rings because of the relatively small range of Δ^{199}Hg between ambient and polluted regions (Blum et al., 2014; Sun et al., 2019). Secondly, Δ^{199}Hg between tree rings and atmosphere may not follow a linear correlation due to Hg re-emission from foliage, which would induce *a* ~0.1‰ negative shift in foliage (Demers et al., 2013; Yuan et al., 2019). Finally, the radial translocation may cause the previously Hg isotopic signatures mixed with new signals at high resolution, thus obscuring the true atmospheric Hg isotopic signals (Wang et al., 2021b).

7. Summary and future directions for Hg dendrochemistry

The tree-ring Hg records in remote regions have been successfully used to reconstruct the peak of anthropogenic Hg emissions in Europe and North America in 1960s-1970s and the distinct increase of Hg emissions in Asia since 1980s. Tree rings provide an opportunity to understand the impact of human activities on historical atmospheric Hg cycling, which may play an important role in assessing the effectiveness of the Minamata Convention on controlling Hg pollution.

Hg accumulation in bole wood is suggested to be dominated by translocation of foliage Hg through phloem transportation. The active transport of ray cells in the sapwood controls the radial Hg translocation in tree rings. Impacts of radial translocation on tree-ring Hg records are species-specific. The tree physiological factors and environmental conditions significantly influence Hg accumulation and translocation in tree rings. The knowledge gaps for Hg sources and translocation, specifically the bark absorption and radial translocation of Hg in sapwood tree rings, lead to difficulties in evaluating the tree-ring Hg records. To improve reliability of Hg dendrochemistry, we recommend several issues as follows.

1. **Understanding the Hg isotopic fractionation in tree to further elucidate the Hg sources and translocation processes in tree rings.** Hg isotopes provide new insights in identifying Hg sources and understanding the biogeochemical processes. However, the knowledge gaps in Hg isotopic fractionation during the translocation within trees constrain our capability in tracing Hg translocation processes and source contributions. Additionally, knowing that the atmospheric Hg^0 is the dominant source of Hg accumulation in tree rings, it is still unclear whether the elevated Hg concentration in tree rings near the bark is caused by the bark Hg lateral translocation.
2. **Understanding tree physiological and environmental impacts on tree-ring Hg variations by controlled network experiments.** Due to the complicated coupling effects from environmental and tree physiological factors on tree-ring Hg variations, the Hg profiles in tree rings exhibit high variabilities within intra-tree and between species and sites. We recommend to quantify impacts of physiological conditions and tree canopy dynamics (tree species, age and height) and environmental factors (e.g., meteorological factors, and geographical and geomorphological conditions) by setting up the tree-ring Hg monitoring

network along the elevation and gradient of environmental factors or atmospheric Hg^0 concentrations.

3. **Using various statistical models to display relations between atmospheric Hg and tree-ring Hg signatures.** Various statistical models based the big data of geographical and geomorphological conditions, meteorology indicators, tree age and species, etc., would help quantify the nonlinear relationship of $Hg_{tree} * f(r) = Hg_{air}$, thus reducing the uncertainties of tree-ring records. Furthermore, using the combination of tree-ring Hg concentrations and Hg isotopic signatures (δ^{202}Hg, Δ^{199}Hg, Δ^{200}Hg, Δ^{201}Hg, Δ^{204}Hg) would comprehensively reconstruct the historical Hg trends at multi-dimension of Hg contents, sources and processes.

Disclosure statement

The authors declare no competing financial interest.

Funding

This work was funded by National Natural Science Foundation of China [42122053 and 41977272] and Natural Science Foundation of Chongqing [cstc2020jcyj-msxmX0063].

ORCID

Xun Wang http://orcid.org/0000-0002-7407-8965

References

Abreu, S. N., Soares, A. M. V. M., Nogueira, A. J. A., & Morgado, F. (2008). Tree rings, populus nigra l., as mercury data logger in aquatic environments: Case study of an historically contaminated environment. *Bulletin of Environmental Contamination and Toxicology*, *80*(3), 294–299.

Ahn, Y. S., Jung, R., & Moon, J.-H. (2020). Approaches to understand historical changes of mercury in tree rings of Japanese Cypress in Industrial Areas. *Forests*, *11*(8), 800.

Arnold, J., Gustin, M. S., & Weisberg, P. J. (2018). Evidence for nonstomatal uptake of Hg by Aspen and translocation of Hg from foliage to tree rings in Austrian pine. *Environmental Science & Technology*, *52*(3), 1174–1182.

Assad, M., Parelle, J., Cazaux, D., Gimbert, F., Chalot, M., & Tatin-Froux, F. (2016). Mercury uptake into poplar leaves. *Chemosphere*, *146*, 1–7.

Beckers, F., & Rinklebe, J. (2017). Cycling of mercury in the environment: Sources, fate, and human health implications: A review. *Critical Reviews in Environmental Science and Technology*, *47*(9), 693–794.

Bishop, K. H., Lee, Y. H., Munthe, J., & Dambrine, E. (1998). Xylem sap as a pathway for total mercury and methylmercury transport from soils to tree canopy in the boreal forest. *Biogeochemistry*, *40*(2/3), 101–113.

Blum, J. D., & Bergquist, B. A. (2007). Reporting of variations in the natural isotopic composition of mercury. *Analytical and Bioanalytical Chemistry*, *388*(2), 353–359.

Blum, J. D., Sherman, L. S., & Johnson, M. W. (2014). Mercury isotopes in earth and environmental sciences. *Annual Review of Earth and Planetary Sciences*, *42*(1), 249–269.

Boszke, L., Kowalski, A., Astel, A., Barański, A., Gworek, B., & Siepak, J. (2008). Mercury mobility and bioavailability in soil from contaminated area. *Environmental Geology*, *55*(5), 1075–1087.

Carrasco-Gil, S., Siebner, H., Leduc, D. L., Webb, S. M., Millan, R., Andrews, J. C., & Hernandez, L. E. (2013). Mercury localization and speciation in plants grown hydroponically or in a natural environment. *Environmental Science & Technology*, *47*(7), 3082–3090.

Chellman, N., Csank, A., Gustin, M. S., Arienzo, M. M., Vargas Estrada, M., & McConnell, J. R. (2020). Comparison of co-located ice-core and tree-ring mercury records indicates potential radial translocation of mercury in whitebark pine. *The Science of the Total Environment*, *743*, 140695.

Chen, C. Y., Driscoll, C. T., Eagles-Smith, C. A., Eckley, C. S., Gay, D. A., Hsu-Kim, H., Keane, S. E., Kirk, J. L., Mason, R. P., Obrist, D., Selin, H., Selin, N. E., & Thompson, M. R. (2018). A critical time for mercury science to inform global policy. *Environmental Science & Technology*, *52*(17), 9556–9561.

Chen, L., Wang, H. H., Liu, J. F., Tong, Y. D., Ou, L. B., Zhang, W., Hu, D., Chen, C., & Wang, X. J. (2014). Intercontinental transport and deposition patterns of atmospheric mercury from anthropogenic emissions. *Atmospheric Chemistry and Physics*, *14*(18), 10163–10176.

Cheng, Z., Buckley, B. M., Katz, B., Wright, W., Bailey, R., Smith, K. T., Li, J., Curtis, A., & Geen, A. (2007). Arsenic in tree rings at a highly contaminated site. *The Science of the Total Environment*, *376*(1-3), 324–334.

Chiarantini, L., Rimondi, V., Benvenuti, M., Beutel, M. W., Costagliola, P., Gonnelli, C., Lattanzi, P., & Paolieri, M. (2016). Black pine (pinus nigra) barks as biomonitors of airborne mercury pollution. *The Science of the Total Environment*, *569-570*, 105–113.

Chiarantini, L., Rimondi, V., Bardelli, F., Benvenuti, M., Cosio, C., Costagliola, P., Di Benedetto, F., Lattanzi, P., & Sarret, G. (2017). Mercury speciation in pinus nigra barks from Monte Amiata (Italy): An X-ray absorption spectroscopy study. *Environmental Pollution (Barking, Essex: 1987)*, *227*, 83–88.

Clackett, S. P., Porter, T. J., & Lehnherr, I. (2018). 400-year record of atmospheric mercury from tree-rings in northwestern Canada. *Environmental Science & Technology*, *52*(17), 9625–9633.

Clackett, S. P., Porter, T. J., & Lehnherr, I. (2021). The tree-ring mercury record of Klondike gold mining at Bear Creek, central Yukon. *Environmental Pollution (Barking, Essex: 1987)*, *268*(Pt B), 115777.

Converse, A. D., Riscassi, A. L., & Scanlon, T. M. (2010). Seasonal variability in gaseous mercury fluxes measured in a high-elevation meadow. *Atmospheric Environment*, *44*(18), 2176–2185.

Cook, E. R., Shiyatov, S., & Mazepa, V. (1990). Estimation of the mean chronology. In: Fritts H.C., Guiot J., Gordon G. A., eds. *Methods of dendrochronology-applications in the environmental sciences*. Academic Publishers.

Cooke, C. A., Martinez-Cortizas, A., Bindler, R., & Sexauer Gustin, M. (2020). Environmental archives of atmospheric Hg deposition - a review. *The Science of the Total Environment*, *709*, 134800.

Cui, L. W., Feng, X. B., Lin, C.-J., Wang, X. M., Meng, B., Wang, X., & Wang, H. (2014). Accumulation and translocation of 198Hg in four crop species. *Environmental Toxicology and Chemistry*, *33*(2), 334–340.

Cutter, B. E., & Guyette, R. P. (1993). Anatomical, chemical, and ecological factors affecting tree species choice in dendrochemistry studies. *Journal of Environmental Quality*, *22*(3), 611–619.

Demers, J. D., Blum, J. D., & Zak, D. R. (2013). Mercury isotopes in a forested ecosystem: Implications for air-surface exchange dynamics and the global mercury cycle. *Global Biogeochemical Cycles*, *27*(1), 222–238.

Eccles, K. M., Majeed, H., Porter, T. J., & Lehnherr, I. (2020). A continental and marine-influenced tree-ring mercury record in the old crow flats, Yukon, Canada. *ACS Earth and Space Chemistry*, *4*(8), 1281–1290.

England, J. R., & Attiwill, P. M. (2006). Changes in leaf morphology and anatomy with tree age and height in the broadleaved evergreen species, Eucalyptus regnans F. Muell. *Trees*, *20*(1), 79–90.

Engstrom, D. R., Fitzgerald, W. F., Cooke, C. A., Lamborg, C. H., Drevnick, P. E., Swain, E. B., Balogh, S. J., & Balcom, P. H. (2014). Atmospheric Hg emissions from preindustrial gold and silver extraction in the Americas: A reevaluation from lake-sediment archives. *Environmental Science & Technology*, *48*(12), 6533–6543.

Enrico, M., Le Roux, G., Heimburger, L. E., Van Beek, P., Souhaut, M., Chmeleff, J., & Sonke, J. E. (2017). Holocene atmospheric mercury levels reconstructed from peat bog mercury stable isotopes. *Environmental Science & Technology*, *51*(11), 5899–5906.

Enrico, M., Roux, G. L., Marusczak, N., Heimburger, L. E., Claustres, A., Fu, X., Sun, R., & Sonke, J. E. (2016). Atmospheric mercury transfer to peat bogs dominated by gaseous elemental mercury dry deposition. *Environmental Science & Technology*, *50*(5), 2405–2412.

Evans, M., Muir, D., Brua, R. B., Keating, J., & Wang, X. (2013). Mercury trends in predatory fish in great slave lake: The influence of temperature and other climate drivers. *Environmental Science & Technology*, *47*(22), 12793–12801.

Eyrikh, S., Eichler, A., Tobler, L., Malygina, N., Papina, T., & Schwikowski, M. (2017). A 320 year ice-core record of atmospheric Hg pollution in the Altai, central Asia. *Environmental Science & Technology*, *51*(20), 11597–11606.

Fleck, J. A., Grigal, D. F., & Nater, E. A. (1999). Mercury uptake by trees: An observational experiment. *Water, Air, and Soil Pollution*, *115*(1/4), 513–523.

Frescholtz, T. F. G., M. S., Schorran, D. E., & Fernandez, G. C. J. (2003). Assessing the source of mercury in foliar tissue of quaking Aspen. *Environmental Toxicology and Chemistry*, *22*(9), 2114–2119.

Fu, X., Jiskra, M., Yang, X., Marusczak, N., Enrico, M., Chmeleff, J., Heimburger-Boavida, L. E., Gheusi, F., & Sonke, J. E. (2021). Mass-independent fractionation of even and odd mercury isotopes during atmospheric mercury redox reactions. *Environmental Science & Technology*, *55*(14), 10164–10174.

Fu, X. W., F, X., Dong, Z. Q., Yin, R. S., Wang, J. X., Yang, Z. R., & Zhang, H. (2010). Atmospheric gaseous elemental mercury (gem) concentrations and mercury depositions at a high-altitude mountain peak in south China. *Atmospheric Chemistry and Physics*, *10*(5), 2425–2437.

Ghotra, A., Lehnherr, I., Porter, T. J., & Pisaric, M. F. J. (2020). Tree-ring inferred atmospheric mercury concentrations in the Mackenzie Delta (NWT, Canada) peaked in the 1970s but are increasing once more. *ACS Earth and Space Chemistry*, *4*(3), 457–466.

Graydon, J. A., St Louis, V. L., Hintelmann, H., Lindberg, S. E., Sandilands, K. A., Rudd, J. W., Kelly, C. A., Tate, M. T., Krabbenhoft, D. P., & Lehnherr, I. (2009). Investigation of uptake and retention of atmospheric Hg(ii) by boreal forest plants using stable Hg isotopes. *Environmental Science & Technology*, *43*(13), 4960–4966.

Greger, M., Wang, Y., & Neuschutz, C. (2005). Absence of Hg transpiration by shoot after Hg uptake by roots of six terrestrial plant species. *Environmental Pollution (Barking, Essex: 1987)*, *134*(2), 201–208.

Guedron, S., Amouroux, D., Tessier, E., Grimaldi, C., Barre, J., Berail, S., Perrot, V., & Grimaldi, M. (2018). Mercury isotopic fractionation during pedogenesis in a tropical forest soil catena (French Guiana): Deciphering the impact of historical gold mining. *Environmental Science & Technology*, *52*(20), 11573–11582.

Guerrero, S. (2016). The history of silver refining in New Spain, 16c to 18c: Back to the basics. *History and Technology*, *32*(1), 2–32.

Gustin, M. S., Ingle, B., & Dunham-Cheatham, S. M. (2022a). Further investigations into the use of tree rings as archives of atmospheric mercury concentrations. *Biogeochemistry*, *158*(2), 167–180.

Gustin, M. S., Dunham-Cheatham, S. M., Harper, J. F., Choi, W. G., Blum, J. D., & Johnson, M. W. (2022b). Investigation of the biochemical controls on mercury uptake and mobility in trees. *The Science of the Total Environment*, *851*(Pt 1), 158101.

Hagemeyer, J., & Schafer, H. (1995). Seasonal variations in concentrations and radial distribution patterns of Cd, Pb and Zn in stem wood of beech trees (Fagus sylvatica L.). *Science of the Total Environment*, *166*(1-3), 77–87.

Hojdová, M., Navrátil, T., Rohovec, J., Žák, K., Vaněk, A., Chrastný, V., Bače, R., & Svoboda, M. (2011). Changes in mercury deposition in a mining and smelting region as recorded in tree rings. *Water, Air, & Soil Pollution*, *216*(1-4), 73–82.

Horowitz, H. M., Jacob, D. J., Amos, H. M., Streets, D. G., & Sunderland, E. M. (2014). Historical mercury releases from commercial products: Global environmental implications. *Environmental Science & Technology*, *48*(17), 10242–10250.

Hubbard, R. M., Bond, B. J., & Ryan, M. G. (1999). Evidence that hydraulic conductance limits photosynthesis in old Pinus ponderosa trees. *Tree Physiology*, *19*(3), 165–172.

Jung, R., & Ahn, Y. S. (2017). Distribution of mercury concentrations in tree rings and surface soils adjacent to a phosphate fertilizer plant in southern Korea. *Bulletin of Environmental Contamination and Toxicology*, *99*(2), 253–257.

Kang, H., Liu, X., Guo, J., Zhang, Q., Wang, Y., Huang, J., Xu, G., Wu, G., Ge, W., & Kang, S. (2022). Long-term mercury variations in tree rings of the permafrost forest, northeastern China. *Science China Earth Sciences*, *65*(7), 1328–1338.

Kang, H. H., Liu, X. H., Guo, J. M., Xu, G. B., Wu, G. J., Zeng, X. M., Wang, B., & Kang, S. C. (2018). Increased mercury pollution revealed by tree rings from the China's Tianshan Mountains. *Science Bulletin*, *63*(20), 1328–1331.

Kang, H. H., Liu, X. H., Guo, J. M., Wang, B., Xu, G. B., Wu, G. J., Kang, S. C., & Huang, J. (2019). Characterization of mercury concentration from soils to needle and tree rings of Schrenk spruce (Picea schrenkiana) of the middle Tianshan Mountains, northwestern China. *Ecological Indicators*, *104*, 24–31.

Kang, S. C., Huang, J., Wang, F. Y., Zhang, Q. G., Zhang, Y. L., Li, C. L., Wang, L., Chen, P. F., Sharma, C. M., Li, Q., Sillanpaa, M., Hou, J. Z., Xu, B. Q., & Guo, J. M. (2016). Atmospheric mercury depositional chronology reconstructed from lake sediments and ice core in the Himalayas and Tibetan Plateau. *Environmental Science & Technology*, *50*(6), 2859–2869.

Kwon, S. Y., Blum, J. D., Yin, R., Tsui, M. T.-K., Yang, Y. H., & Choi, J. W. (2020). Mercury stable isotopes for monitoring the effectiveness of the minamata convention on mercury. *Earth-Science Reviews*, *203*, 103111.

Laacouri, A., Nater, E. A., & Kolka, R. K. (2013). Distribution and uptake dynamics of mercury in leaves of common deciduous tree species in Minnesota, u.S.A. *Environmental Science & Technology*, *47*(18), 10462–10470.

Lageard, J. G., Howell, J. A., Rothwell, J. J., & Drew, I. B. (2008). The utility of pinus sylvestris l. In dendrochemical investigations: Pollution impact of lead mining and smelting in darley dale, derbyshire, uk. *Environmental Pollution (Barking, Essex: 1987)*, *153*(2), 284–294.

Lehnherr, I. (2014). Methylmercury biogeochemistry: A review with special reference to Arctic aquatic ecosystems. *Environmental Reviews*, *22*(3), 229–243.

Liu, X., Wang, X., & Wang, D. (2024). Assessment of tree-ring mercury radial translocation and age effect in masson pine: Implications for historical atmospheric mercury reconstruction. *Journal of Environmental Sciences*, *138*, 266–276.

Liu, Y., Liu, G., Wang, Z., Guo, Y., Yin, Y., Zhang, X., Cai, Y., & Jiang, G. (2021a). Understanding foliar accumulation of atmospheric Hg in terrestrial vegetation: Progress and challenges. *Critical Reviews in Environmental Science and Technology*, *52*(24), 4331–4352.

Liu, Y., Tao, H., Wang, Y., Fang, Y., Xiang, Y., Liu, G., Guo, Y., Liu, J., Yin, Y., Cai, Y., & Jiang, G. (2021b). Gaseous elemental mercury [Hg(0)] oxidation in poplar leaves through a two-step single-electron transfer process. *Environmental Science & Technology Letters*, *8*(12), 1098–1103.

Lu, Z., Yuan, W., Luo, K., & Wang, X. (2021). Litterfall mercury reduction on a subtropical evergreen broadleaf forest floor revealed by multi-element isotopes. *Environmental Pollution (Barking, Essex: 1987)*, *268*(Pt A), 115867.

Maillard, F., Girardclos, O., Assad, M., Zappelini, C., Perez Mena, J. M., Yung, L., Guyeux, C., Chretien, S., Bigham, G., Cosio, C., & Chalot, M. (2016). Dendrochemical assessment of mercury releases from a pond and dredged-sediment landfill impacted by a chlor-alkali plant. *Environmental Research*, *148*, 122–126.

Manceau, A., Wang, J., Rovezzi, M., Glatzel, P., & Feng, X. (2018). Biogenesis of mercury-sulfur nanoparticles in plant leaves from atmospheric gaseous mercury. *Environmental Science & Technology*, *52*(7), 3935–3948.

Mao, Y., Li, Y., Richards, J., & Cai, Y. (2013). Investigating uptake and translocation of mercury species by sawgrass (Cladium jamaicense) using a stable isotope tracer technique. *Environmental Science & Technology*, *47*(17), 9678–9684.

McLagan, D. S., Biester, H., Navrátil, T., Kraemer, S. M., & Schwab, L. (2022). Internal tree cycling and atmospheric archiving of mercury: Examination with concentration and stable isotope analyses. *Biogeosciences*, *19*(17), 4415–4429.

Millhollen, A. G., G, M. S., & Obrist, D. (2006). Foliar mercury accumulation and exchange for three tree species. *Environmental Science & Technology*, *40*(19), 6001–6006.

Navratil, T., Simecek, M., Shanley, J. B., Rohovec, J., Hojdova, M., & Houska, J. (2017). The history of mercury pollution near the Spolana chlor-alkali plant (Neratovice, Czech Republic) as recorded by Scots pine tree rings and other bioindicators. *The Science of the Total Environment*, *586*, 1182–1192.

Navrátil, T., Nováková, T., Shanley, J. B., Rohovec, J., Matoušková, Š., Vaňková, M., & Norton, S. A. (2018). Larch tree rings as a tool for reconstructing 20th century central European atmospheric mercury trends. *Environmental Science & Technology*, *52*(19), 11060–11068.

Novakova, T., Navratil, T., Demers, J. D., Roll, M., & Rohovec, J. (2021). Contrasting tree ring Hg records in two conifer species: Multi-site evidence of species-specific radial translocation effects in Scots pine versus European larch. *The Science of the Total Environment*, *762*, 144022.

Novakova, T., Navratil, T., Schutze, M., Rohovec, J., Matouskova, S., Hosek, M., & Matys Grygar, T. (2022). Reconstructing atmospheric Hg levels near the oldest chemical factory in central europe using a tree ring archive. *Environmental Pollution (Barking, Essex: 1987)*, *304*, 119215.

Okada, N., Hirakawa, Y., & Katayama, Y. (2012). Radial movement of sapwood-injected rubidium into heartwood of Japanese cedar (Cryptomeria japonica) in the growing period. *Journal of Wood Science*, *58*(1), 1–8.

Pang, Q., Gu, J., Wang, H., & Zhang, Y. (2022). Global health impact of atmospheric mercury emissions from artisanal and small-scale gold mining. *iScience*, *25*(9), 104881.

Peckham, M. A., Gustin, M. S., & Weisberg, P. J. (2019a). Assessment of the suitability of tree rings as archives of global and regional atmospheric mercury pollution. *Environmental Science & Technology*, *53*(7), 3663–3671.

Peckham, M. A., Gustin, M. S., Weisberg, P. J., & Weiss-Penzias, P. (2019b). Results of a controlled field experiment to assess the use of tree tissue concentrations as bioindicators of air Hg. *Biogeochemistry*, *142*(2), 265–279.

Rodriguez Martin, J. A., Nanos, N., Miranda, J. C., Carbonell, G., & Gil, L. (2013). Volcanic mercury in pinus canariensis. *Die Naturwissenschaften*, *100*(8), 739–747.

Rutter, A. P., Schauer, J. J., Shafer, M. M., Creswell, J., Olson, M. R., Clary, A., Robinson, M., Parman, A. M., & Katzman, T. L. (2011). Climate sensitivity of gaseous elemental mercury dry deposition to plants: Impacts of temperature, light intensity, and plant species. *Environmental Science & Technology*, *45*(2), 569–575.

Scanlon, T. M., Riscassi, A. L., Demers, J. D., Camper, T. D., Lee, T. R., & Druckenbrod, D. L. (2020). Mercury accumulation in tree rings: Observed trends in quantity and isotopic composition in Shenandoah National Park, Virginia. *Journal of Geophysical Research: Biogeosciences*, *125*(2)

Schneider, L., Allen, K., Walker, M., Morgan, C., & Haberle, S. (2019). Using tree rings to track atmospheric mercury pollution in Australia: The legacy of mining in Tasmania. *Environmental Science & Technology*, *53*(10), 5697–5706.

Schreiber, L. (2005). Polar paths of diffusion across plant cuticles: New evidence for an old hypothesis. *Annals of Botany*, *95*(7), 1069–1073.

Schuster, P. F., K, D. P., Naftz, D. L., Cecil, L. D., Olson, M. L., Dewild, J. F., Susong, D. D., Green, J. R., & Abbott, M. L. (2002). Atmospheric mercury deposition during the last 270 years: A glacial ice core record of natural and anthropogenic sources. *Environmental Science & Technology*, *36*(11), 2303–2310.

Schwarz, P. A., Fahey, T. J., & Dawson, T. E. (1997). Seasonal air and soil temperature effects on photosynthesis in red spruce (Picea rubens) saplings. *Tree Physiology*, *17*(3), 187–194.

Selin, H., & Selin, N. E. (2022). From stockholm to minamata and beyond: Governing mercury pollution for a more sustainable future. *One Earth*, *5*(10), 1109–1125.

Şen, A., Pereira, H., Olivella, M. A., & Villaescusa, I. (2015). Heavy metals removal in aqueous environments using bark as a biosorbent. *International Journal of Environmental Science and Technology*, *12*(1), 391–404.

Shah, V., Jacob, D. J., Thackray, C. P., Wang, X., Sunderland, E. M., Dibble, T. S., Saiz-Lopez, A., Černušák, I., Kellö, V., Castro, P. J., Wu, R., & Wang, C. (2021). Improved mechanistic model of the atmospheric redox chemistry of mercury. *Environmental Science & Technology*, *55*(21), 14445–14456.

Siwik, E. I., Campbell, L. M., & Mierle, G. (2010). Distribution and trends of mercury in deciduous tree cores. *Environmental Pollution (Barking, Essex: 1987)*, *158*(6), 2067–2073.

Sonke, J. E., & Blum, J. D. (2013). Advances in mercury stable isotope biogeochemistry. *Chemical Geology*, *336*, 1–4.

Sonke, J. E., Angot, H., Zhang, Y., Poulain, A., Bjorn, E., & Schartup, A. (2023). Global change effects on biogeochemical mercury cycling. *Ambio*, *52*(5), 853–876.

Stamenkovic, J., & Gustin, M. S. (2009). Nonstomatal versus stomatal uptake of atmospheric mercury. *Environmental Science & Technology*, *43*(5), 1367–1372.

Stewart, C. M. (1966). Excretion and hearthwood formation in living trees. *Science (New York, N.Y.)*, *153*(3740), 1068–1074.

Stoffberg, G. H., van Rooyen, M. W., van der Linde, M. J., & Groeneveld, H. T. (2008). Predicting the growth in tree height and crown size of three street tree species in the City of Tshwane, South Africa. *Urban Forestry & Urban Greening*, *7*(4), 259–264.

Streets, D. G., Devane, M. K., Lu, Z., Bond, T. C., Sunderland, E. M., & Jacob, D. J. (2011). All-time releases of mercury to the atmosphere from human activities. *Environmental Science & Technology*, *45*(24), 10485–10491.

Streets, D. G., Horowitz, H. M., Jacob, D. J., Lu, Z., Levin, L., Ter Schure, A. F. H., & Sunderland, E. M. (2017). Total mercury released to the environment by human activities. *Environmental Science & Technology*, *51*(11), 5969–5977.

Sun, R., Jiskra, M., Amos, H. M., Zhang, Y., Sunderland, E. M., & Sonke, J. E. (2019). Modelling the mercury stable isotope distribution of earth surface reservoirs: Implications for global Hg cycling. *Geochimica et Cosmochimica Acta*, *246*, 156–173.

UNEP. (2019). *Global mercury assessment 2018. UNEP*. Chemicals and Health Branch.

Wang, J. J., Guo, Y. Y., Guo, D. L., Yin, S. L., Kong, D. L., Liu, Y. S., & Zeng, H. (2012). Fine root mercury heterogeneity: Metabolism of lower-order roots as an effective route for mercury removal. *Environmental Science & Technology*, *46*(2), 769–777.

Wang, X., Yuan, W., Lin, C.-J., & Feng, X. B. (2021a). Mercury cycling and isotopic fractionation in global forests. *Critical Reviews in Environmental Science and Technology*, *52*(21), 3763–3786.

Wang, X., Yuan, W., Lin, C.-J., Wu, F., & Feng, X. B. (2021b). Stable mercury isotopes stored in Masson Pinus tree rings as atmospheric mercury archives. *Journal of Hazardous Materials*, *415*, 125678.

Wang, X., Yuan, W., Lin, C.-J., Luo, J., Wang, F. Y., Feng, X. B., Fu, X. W., & Liu, C. (2020a). Underestimated sink of atmospheric mercury in a deglaciated forest chronosequence. *Environmental Science & Technology*, *54*(13), 8083–8093.

Wang, X., Luo, J., Yuan, W., Lin, C. J., Wang, F., Liu, C., Wang, G., & Feng, X. (2020b). Global warming accelerates uptake of atmospheric mercury in regions experiencing glacier retreat. *Proceedings of the National Academy of Sciences of the United States of America*, *117*(4), 2049–2055.

Watmough, S. A., & Hutchinson, T. C. (2002). Historical changes in lead concentrations in tree-rings of sycamore, oak and Scots pine in north-west England. *The Science of the Total Environment*, *293*(1-3), 85–96.

Wohlgemuth, L., Rautio, P., Ahrends, B., Russ, A., Vesterdal, L., Waldner, P., Timmermann, V., Eickenscheidt, N., Fürst, A., Greve, M., Roskams, P., Thimonier, A., Nicolas, M., Kowalska, A., Ingerslev, M., Merilä, P., Benham, S., Iacoban, C., Hoch, G., Alewell, C., & Jiskra, M. (2022). Physiological and climate controls on foliar mercury uptake by European tree species. *Biogeosciences*, *19*(5), 1335–1353.

Wright, G., Woodward, C., Peri, L., Weisberg, P. J., & Gustin, M. S. (2014). Application of tree rings [dendrochemistry] for detecting historical trends in air Hg concentrations across multiple scales. *Biogeochemistry*, *120*(1-3), 149–162.

Wu, Q. R., Wang, S. X., Li, G. L., Liang, S., Lin, C.-J., Wang, Y. F., Cai, S. Y., Liu, K. Y., & Hao, J. M. (2016). Temporal trend and spatial distribution of speciated atmospheric mercury emissions in China during 1978-2014. *Environmental Science & Technology*, *50*(24), 13428–13435.

Yanai, R. D., Yang, Y., Wild, A. D., Smith, K. T., & Driscoll, C. T. (2020). New approaches to understand mercury in trees: Radial and longitudinal patterns of mercury in tree rings and genetic control of mercury in maple sap. *Water, Air, & Soil Pollution*, *231*(5), 1–10.

Yu, B., Yang, L., Liu, H., Xiao, C., Bu, D., Zhang, Q., Fu, J., Zhang, Q., Cong, Z., Liang, Y., Hu, L., Yin, Y., Shi, J., & Jiang, G. (2022). Tracing the transboundary transport of mercury to the Tibetan Plateau using atmospheric mercury isotopes. *Environmental Science & Technology*, *56*(3), 1568–1577.

Yuan, W., Wang, X., Lin, C.-J., Wu, F., Luo, K., Zhang, H., Lu, Z., & Feng, X. (2022). Mercury uptake, accumulation, and translocation in roots of subtropical forest: Implications of global mercury budget. *Environmental Science & Technology*, *56*(19), 14154–14165.

Yuan, W., Sommar, J., Lin, C. J., Wang, X., Li, K., Liu, Y., Zhang, H., Lu, Z., Wu, C., & Feng, X. (2019). Stable isotope evidence shows re-emission of elemental mercury vapor occurring after reductive loss from foliage. *Environmental Science & Technology*, *53*(2), 651–660.

Zhang, H., Fu, X. W., Lin, C. J., Wang, X., & Feng, X. B. (2015). Observation and analysis of speciated atmospheric mercury in shangri-la, Tibetan Plateau, China. *Atmospheric Chemistry and Physics*, *15*(2), 653–665.

Zhang, L. M., Wright, L. P., & Blanchard, P. (2009). A review of current knowledge concerning dry deposition of atmospheric mercury. *Atmospheric Environment*, *43*(37), 5853–5864.

Zhang, Q., Pan, K., Kang, S., Zhu, A., & Wang, W. X. (2014). Mercury in wild fish from high-altitude aquatic ecosystems in the Tibetan Plateau. *Environmental Science & Technology*, *48*(9), 5220–5228.

Zhang, Y., Chen, J., Zheng, W., Sun, R., Yuan, S., Cai, H., Yang, D. A., Yuan, W., Meng, M., Wang, Z., Liu, Y., & Liu, J. (2020). Mercury isotope compositions in large anthropogenically impacted pearl river, south China. *Ecotoxicology and Environmental Safety*, *191*, 110229.

Zheng, W., Obrist, D., Weis, D., & Bergquist, B. A. (2016). Mercury isotope compositions across north american forests. *Global Biogeochemical Cycles*, *30*(10), 1475–1492.

Zhou, J., & Obrist, D. (2021). Global mercury assimilation by vegetation. *Environmental Science & Technology*, *55*(20), 14245–14257.

Zuna, M., Ettler, V., Sebek, O., & Mihaljevic, M. (2012). Mercury accumulation in peatbogs at Czech sites with contrasting pollution histories. *The Science of the Total Environment*, *424*, 322–330.